Bioorganic & Medicinal Chemistry 20 (2012) 4437–4442

Contents lists available at SciVerse ScienceDirect

Bioorganic & Medicinal Chemistry

journal homepage: www.elsevier.com/locate/bmc

Hyrtioreticulins A–E, indole alkaloids inhibiting the ubiquitin-activating enzyme, from the marine sponge *Hyrtios reticulatus*

Rumi Yamanokuchi [a,†], Kumiko Imada [a,†], Mitsue Miyazaki [a], Hikaru Kato [a], Tadashi Watanabe [b], Masahiro Fujimuro [b], Yasushi Saeki [c], Sosuke Yoshinaga [a], Hiroaki Terasawa [a], Noriyuki Iwasaki [d], Henki Rotinsulu [e,f], Fitje Losung [g], Remy E. P. Mangindaan [g], Michio Namikoshi [e], Nicole J. de Voogd [h], Hideyoshi Yokosawa [i], Sachiko Tsukamoto [a,*]

[a] *Graduate School of Pharmaceutical Sciences, Kumamoto University, Kumamoto 862-0973, Japan*
[b] *Kyoto Pharmaceutical University, 1 Misasagi-shichono-cho, Yamashina-ku, Kyoto 607-8412, Japan*
[c] *Tokyo Metropolitan Institute of Medical Science, 2-1-6 Kamikitazawa, Setagaya-ku, Tokyo 156-8506, Japan*
[d] *Bruker Daltonics K.K., 3-9 Moriya, Kanagawa-ku, Yokohama 221-0022, Japan*
[e] *Tohoku Pharmaceutical University, Aoba-ku, Sendai 981-8558, Japan*
[f] *Faculty of Agriculture, Universitas Pembangunan Indonesia, Manado 95361, Indonesia*
[g] *Faculty of Fisheries and Marine Science, Sam Ratulangi University, Kampus Bahu, Manado 95115, Indonesia*
[h] *Netherlands Centre for Biodiversity Naturalis, PO Box 9517, 2300 RA Leiden, The Netherlands*
[i] *School of Pharmacy, Aichi Gakuin University, Chikusa-ku, Nagoya 464-8650, Japan*

ARTICLE INFO

Article history:
Received 24 March 2012
Revised 14 May 2012
Accepted 14 May 2012
Available online 24 May 2012

Keywords:
Ubiquitin-activating enzyme inhibitor
Indole alkaloid
Hyrtios reticulatus
Marine sponge

ABSTRACT

Hyrtioreticulins A–E (**1**–**5**) were isolated from the marine sponge *Hyrtios reticulatus*, along with a known alkaloid, hyrtioerectine B (**6**). Structural elucidation on the basis of spectral data showed that **1**, **2**, and **5** are new tetrahydro-β-carboline alkaloids, while **3** and **4** are new azepinoindole-type alkaloids. Hyrtioreticulins A and B (**1** and **2**) inhibited ubiquitin-activating enzyme (E1) with IC_{50} values of 0.75 and 11 μg/mL, respectively, measured by their inhibitory abilities against the formation of an E1-ubiquitin intermediate. So far, only five E1 inhibitors, panapophenanthrine, himeic acid A, largazole, and hyrtioreticulins A and B (**1** and **2**), have been isolated from natural sources and, among them, **1** is the most potent E1 inhibitor.

1. Introduction

Regulated protein degradation via the ubiquitin–proteasome pathway is an essential aspect of various cellular events including cell-cycle control, transcription, and development.[1,2] The ubiquitin–proteasome pathway consists of the ubiquitin system and the 26S proteasome, a proteolytic machine.[1–6] Ubiquitin is composed of 76 amino acids and attaches to a client protein prior to degradation. In the ubiquitin system, ubiquitination requires the sequential actions of three enzymes, ubiquitin-activating enzyme (E1), ubiquitin-conjugating enzyme (E2), and ubiquitin–protein ligase (E3), which result in the formation of the polyubiquitin chain. Ubiquitin is first activated by E1 and linked to its active cysteine residue. The activated ubiquitin is transferred to the active cysteine residue in E2 and then to client proteins, mediated by E3. The formed polyubiquitin chain, tagged to the client protein, is recognized by the 26S proteasome and the protein portion is degraded by it. In 2003, bortezomib (PS-341, Velcade®), a synthetic proteasome inhibitor, was approved for the treatment of relapsed multiple myeloma in the United States, which has opened the way to the discovery of anticancer drugs targeting the proteasome.[7] Since E1 activity is essential for the ubiquitin–proteasome pathway, the development of inhibitors against E1 is another possible route of drug development for the treatment of cancer. In our search for anticancer agents targeting the ubiquitin–proteasome pathway, we isolated himeic acid A from the culture of a marine-derived *Aspergillus* sp. as an E1 inhibitor.[8] Despite many attempts to develop selective E1 inhibitors, only panapophenanthorine,[9] himeic acid A, and largazole[10] have been isolated from natural sources as E1 inhibitors. Recently, a synthetic pyrazone derivative, PYR-41,[11] and a synthetic disulfide compound, NSC624206,[12] were discovered from commercial screening libraries as cell-permeable E1 inhibitors. PYR-41 blocks protein degradation and cytokine-induced activation of NF-κB, activates p53 in cells, and preferentially kills cells transformed with wild-type p53. NSC624206 inhibits p27 ubiquitination. In the continuing search for E1 inhibitors as

* Corresponding author. Tel.: +81 96 371 4380; fax: +81 96 371 4382.
E-mail address: sachiko@kumamoto-u.ac.jp (S. Tsukamoto).
† These authors contributed equally to this work.

0968-0896/$ - see front matter © 2012 Elsevier Ltd. All rights reserved.
http://dx.doi.org/10.1016/j.bmc.2012.05.044

leads for treatment of cancer, we found that an extract of the marine sponge *Hyrtios reticulatus* collected in Indonesia showed significant inhibition of E1 activity. Here, we report the isolation and structural elucidation of new indole alkaloids, hyrtioreticulins A–E (**1**–**5**), along with E1 inhibition by **1** and **2**.

2. Results

2.1. Isolation of hyrtioreticulins A–E

The marine sponge *H. reticulatus* (400 g, wet weight) was collected in Indonesia. The EtOH extract of the sponge was evaporated, and the aqueous residue was extracted with EtOAc and then *n*-BuOH. The *n*-BuOH fraction (9.6 g) was subjected to silica gel and ODS column chromatographies followed by HPLC to afford hyrtioreticulins A (**1**, 4.0 mg), B (**2**, 6.0 mg), C (**3**, 11.0 mg), D (**4**, 20.9 mg), and E (**5**, 10.4 mg), along with hyrtioerectine B[13] (**6**, 255.4 mg) (Fig. 1).

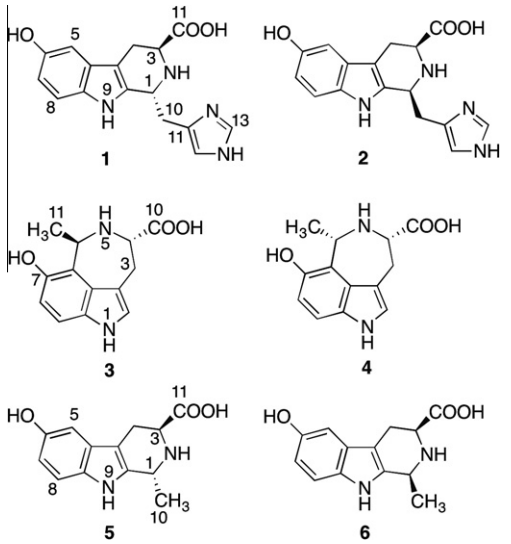

Figure 1. Structures of hyrtioreticulins A–E (**1**–**5**) and hyrtioerectine B (**6**).

2.2. Structural elucidation of hyrtioreticulins A–E (1–5)

The ESIMS of hyrtioreticulin A (**1**) showed a molecular ion peak at *m/z* 313 $[M+H]^+$ and HRESIMS matched a formula of $C_{16}H_{17}N_4O_3$. The ^{1}H NMR spectrum of **1** in CD_3OD (Table 1) showed two methylene groups at δ 3.41 (dd, J = 16.0 and 6.0 Hz)/δ 3.20 (dd, J = 16.0 and 7.7 Hz) and δ 3.55 (2H, m), two methine signals at δ 5.17 (t, J = 6.9 Hz) and δ 4.66 (dd, J = 7.7 and 6.0 Hz), and five aromatic signals at δ 7.15 (d, J = 8.7 Hz), 6.87 (d, J = 1.8 Hz), and 6.74 (dd, J = 8.7 and 1.8 Hz), which accomodated in a 1,2,4-trisubstituted aromatic system, along with two singlet signals at δ 8.86 and 7.36. The ^{13}C NMR spectra showed two methylene carbons at δ 23.5 and 29.4, two methine carbons at δ 49.9 and 52.6, eleven aromatic carbons at δ 103.4 (CH), 106.6 (qC), 113.0 (CH), 113.9 (CH), 118.9 (CH), 128.0 (qC), 129.2 (qC), 130.3 (qC), 133.3 (qC), 136.0 (CH), and 152.2 (qC), and a carbonyl carbon at δ 171.5. The signal at δ 152.2 was indicated to be oxygenated by a chemical shift. Analyses of 2D NMR data suggested that the structure of **1** was similar to that of **6**, except for the absence of a methyl group and the presence of the methylene group (δ_H 3.55 (2H)/δ_C 29.4), two downfield olefinic groups (δ_H 8.86/δ_C 136.0 and δ_H 7.36/δ_C 118.9), and the quaternary carbon (δ_C 130.3). The COSY spectrum showed that the methylene group was attached to C-1 of a tetrahydro-β-carboline unit. The HMBC cross peaks, δ_H 3.55/δ_C 130.3, δ_H 7.36/δ_C 130.3 and 136.0, and δ_H 8.86/δ_C 118.9 and 130.3, indicated that an imidazole ring was attached to the methylene group. Thus, the structure of **1** was a tetrahydro-β-carboline entity with a pendant methylimidazole substituent (Fig. 1). The structure of hyrtioreticulin B (**2**) was indicated to be the same as that of **1** except for the stereochemistry of C-1. The ROESY spectrum of **1** showed the correlation between δ 4.66 (H-3) and δ 3.55 (H-10), which strongly indicated that **1** was the *trans*-configured derivative. Therefore, **2** would be a *cis* isomer, although the ROE or NOE correlation from H-3 was not observed in **2**.

The molecular formulas of hyrtioreticulins C (**3**) and D (**4**), $C_{13}H_{14}N_2O_3$, were the same as that of **6**, as established by FABMS. While the ^{1}H and ^{13}C NMR spectra of **3** and **4** (Table 2) were similar to those of **6**, three aromatic hydrogen atoms of **3** and **4** were observed as two *ortho*-coupling (δ 6.73, d, J = 8.5 Hz and δ 7.15, d, J = 8.5 Hz in **3**) and singlet (δ 7.19 in **3**) signals. The analysis of 2D NMR data for **3** readily indicated that these aromatic hydrogens were accommodated in a 3,4-disubstitued 5-hydroxyindole (indole numbering) nucleus; HMBC correlations, δ_H 6.73 (H-8)/δ_C 114.1 (C-

Table 1
NMR data (500 MHz, CD_3OD) for **1** and **2**

Position	**1**			**2**		
	δ_C	δ_H (J in Hz)	HMBC[a]	δ_C	δ_H (J in Hz	HMBC[a]
1	49.9 CH	5.17 t 6.9	3, 4a, 9a, 10, 11	54.6 CH	5.01 br s	
3	52.6 CH	4.66 dd 7.7, 6.0	1, 4, 4a, 14	59.7 CH	4.26 br d 7.3	
4	23.5 CH_2	3.41 dd 16.0, 6.0	4a, 4b	24.2 CH_2	3.36 m	
		3.20 dd 16.0, 7.7	3, 4a, 4b, 14		3.04 dd 15.1, 12.4	
4a	106.6 qC			107.9 qC		
4b	128.0 qC			128.0 qC		
5	103.4 CH	6.87 d 1.8	4a, 6, 7, 8a	103.4 CH	6.86 d 2.3	6, 8, 8a
6	152.2 qC			152.2 qC		
7	113.9 CH	6.74 dd 8.7, 1.8	5, 6, 8a	113.8 CH	6.75 dd 8.7, 2.3	5, 8a
8	113.0 CH	7.15 d 8.7	4b, 6	113.1 CH	7.22 d 8.7	4b, 6
8a	133.3 qC			133.4 qC		
9a	129.2 qC			129.7 qC		
10	29.4 CH_2	3.55 (2H) m	1, 9a, 11	28.8 CH_2	3.73 br d 14.2	11
					3.36 m	11
11	130.3 qC			130.7 qC		
12	118.9 CH	7.36 s	11, 13	118.6 CH	7.27 s	11, 13
13	136.0 CH	8.86 s	11, 12	136.2 CH	8.73 s	11, 12
14	171.5 qC			170.6 qC		

[a] HMBC correlations are from proton(s) stated for the indicated carbon(s).

Table 2
NMR data (500 MHz, DMSO-d_6) for **3** and **4**

Position	**3**			**4**		
	δ_C	δ_H (J in Hz)	HMBC[a]	δ_C	δ_H (J in Hz	HMBC[a]
1		10.94 s	2, 2a, 9a, 9b		10.83 s	2, 2a, 9a, 9b
2	123.5 CH	7.19 s	2a, 9a, 9b	123.4 CH	7.19 s	2a, 9a, 9b
2a	108.4 qC			101.7 C		
3	28.6 CH_2	3.63 dd 15.6, 1.5	2, 2a, 4, 9b	27.0 CH_2	3.44 dd 16.5, 4.5	2, 2a, 4, 9b
		3.02 dd 15.6, 13.8	2, 2a, 4, 9b		3.36 dd 16.5, 12.5	2, 2a, 4, 9b
4	55.0 CH	4.25 dd 12.8, 1.5	2a, 3, 6, 10	59.9 CH	4.18 dd 12.5, 4.5	10
6	52.0 CH	5.13 q 6.7	4, 6a, 7, 9b, 11	51.7 CH	5.12 q 7.1	4, 6a, 7, 9b, 11
6a	114.1 qC			113.8 qC		
7	145.9 qC			146.4, qC		
8	111.2 CH	6.73 d 8.5	6a, 7, 9a	111.7 CH	6.71 d 8.9	6a, 7, 9a
9	111.2 CH	7.15 d 8.5	7, 9b	111.6 CH	7.14 d 8.9	7, 9b
9a	131.2 qC			130.9 qC		
9b	123.5 qC			125.2 qC		
10	170.5 qC			170.6 qC		
11	16.3 CH_3	1.47 (3H) d 6.7	6, 6a	20.7 CH_3	1.63 (3H) d 7.1	6, 6a
OH-7		9.20 br s			9.13 br s	

[a] HMBC correlations are from proton(s) stated for the indicated carbon(s).

6a), 145.9 (C-7), and 131.2 (C-9a), δ_H 7.15 (H-9)/δ_C 123.5 (C-9b) and 145.9 (C-7), δ_H 7.19 (H-2)/δ_C 108.4 (C-2a), 123.5 (C-9b), and 131.2 (C-9a), and δ_H 10.94 (H-1)/δ_C 108.4 (C-2a), 123.5 (C-2), 123.5 (C-9b), and 131.2 (C-9a). In addition, the presence of a partial structure, –CH_2-CH(COOH)-NH-CH(CH_3)–, which was also accommodated in **6**, was shown by the 2D NMR data for **3**. The HMBC correlations between δ_H 5.13 (H-6) and δ_C 114.1 (C-6a), 123.5 (C-9b), and 145.9 (C-7) and between δ_H 3.02 and 3.63 (H_2-3) and δ_C 108.4 (C-2a), 123.5 (C-2), and 123.5 (C-9b) showed this partial structure to be located at the C-3 and C-4 (indole numbering) positions of the 3,4-disubstitued 5-hydroxyindole nucleus. The ROE correlations, H-4/H_3-11, observed in **3** showed that H-4 and H-6 were on the opposite side. The structure of **4** was indicated to be same as that of **3** except for the stereochemistry of C-6 by the 2D NMR data. The ROESY spectrum of **4** showed a correlation, H-4/H-6, which indicated that these hydrogens were on the same side. Thus, the structures of **3** and **4** were determined as shown in Figure 1.

HRFABMS of hyrtioreticulin E (**5**) showed a molecular formula, $C_{13}H_{14}N_2O_3$, which was the same as those of **3**, **4**, and **6**. ^1H and ^{13}C NMR spectra of **5** in DMSO-d_6 (Table 3) were almost superimposable on those of **6**. The ROESY data showed that the hydrogen atoms at H-3 and H_3-10 were on the same side, while those of **6** were on the opposite side. Synthetic (1*R*,3*S*)- and (1*S*,3*S*)-6-hydroxy-1-methyltetrahydro-β-carboline-3-carboxylic acids showed the characteristic Cotton effects of opposite signs in a 200–250 nm region, that is, the negative Cotton effect for (1*R*,3*S*)-isomer and the positive Cotton effect for (1*S*,3*S*)-isomer,[14] and the CD spectrum of **5** (Fig. 2) matched that of the (1*R*,3*S*)-isomer. Therefore, the absolute configuration of **5** was determined, and biogenetic consideration indicated the 3*S*-configuration for **1**, **2**, and **6** and 4*S*-configuration for **3** and **4**.

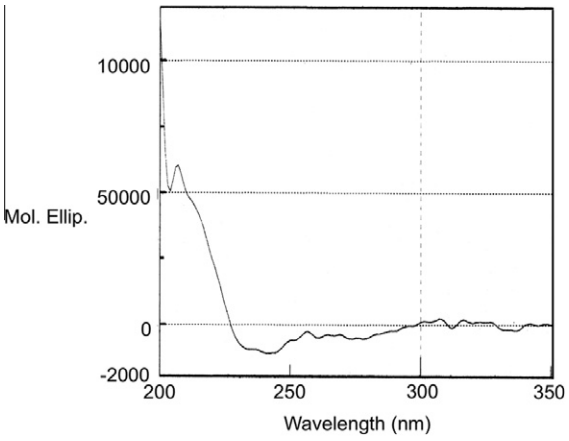

Figure 2. CD spectrum of hyrtioreticulin E (**5**).

Table 3
NMR data (500 MHz, DMSO-d_6) for **5**

Position	δ_C	δ_H (J in Hz)	HMBC[a]
1	47.2 CH	4.70 q 7.0	9a
3	51.4 CH	4.39 dd 8.2, 5.5	11
4	22.1 CH_2	3.12 dd 16.1, 5.5	4a, 9a
		2.95 dd 16.1, 8.2	3, 4a, 9a, 11
4a	103.3 qC		
4b	126.4 qC		
5	102.2 CH	6.74 d 2.2	4a, 6, 7, 8a
6	150.8 qC		
7	111.7 CH	6.62 dd 8.6, 2.2	5, 6, 8a
8	111.9 CH	7.12 d 8.6	4b, 6
8a	130.6 qC		
9		10.78 br s	4a, 4b, 8a, 9a
9a	131.6 qC		
10	17.9 CH_3	1.59 (3H) d 7.0	1, 9a
11	170.2 qC		
OH-6		8.74 br s	

[a] HMBC correlations are from proton(s) stated for the indicated carbon(s).

2.3. Ubiquitin-activating enzyme (E1) inhibition

In an E1-catalyzed ubiquitin-activation reaction, at first, ubiquitin and ATP bind to the respective binding sites of E1, and E1 catalyzes the formation of a ubiquitin–adenylate intermediate and subsequently the binding of ubiquitin to a cysteine residue in the E1 active site in a thiol ester linkage.[15–18] The effects of hyrtioreticulins A–E (**1**–**5**) and hyrtioerectine B (**6**) on the formation of the E1-ubiquitin intermediate from a recombinant FLAG-tagged E1[19] and GST-ubiquitin in the presence of ATP were analyzed by Western blotting with anti-FLAG antibody.[8] Hyrtioreticulins A and B (**1** and **2**) inhibited the E1-ubiquitin intermediate formation (Fig. 3) in a dose-dependent manner with IC_{50} values of 0.75 and 11 μg/mL (2.4 and 35 μM), respectively. Conversely, hyrtioreticulins C–E (**3**–**5**) and hyrtioerectine B (**6**) were unable to block the intermediate formation even at 25 μg/mL (100 μM). The structure-activity relationship among **1**–**6** indicates that the *trans*

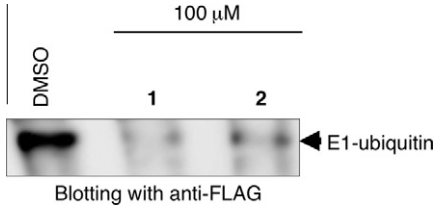

Figure 3. Inhibition of the E1-ubiquitin intermediate formation by **1** and **2**. FLAG-tagged E1, GST-ubiquitin, and ATP were incubated in the presence or absence of 100 μM **1** or **2** in 2% DMSO, and the reaction mixture was subjected to SDS–PAGE, followed by Western blotting with anti-FLAG antibody to detect the E1-ubiquitin intermediate.

configuration at C-1 and the presence of the imidazole ring are required for E1 inhibition.

Immunoprecipitation (IP) experiments (Fig. 4 (A)) with anti-GST antibody-immobilized beads using both GST-ubiquitin and FLAG-tagged E1 in the presence or absence of 50 μM **1**, **2**, and himeic acid A (**7**, Fig. 5) showed that the band corresponding to the immunoprecipitated FLAG-tagged E1 (FLAG-E1) in the presence of **7** was substantially decreased, compared with that in the presence of DMSO only (a control), whereas that in the presence of **1** or **2** remained unchanged. These results strongly suggest that **1** and **2** were unable to inhibit the binding of ubiquitin to the binding site

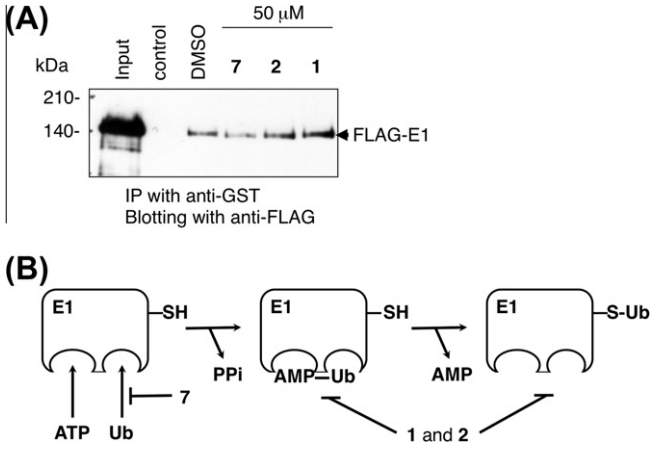

Figure 4. (A) Himeic acid A (**7**), but not hyrtioreticulin A (**1**) or B (**2**), inhibits the binding of ubiquitin to the E1 enzyme. GST-ubiquitin was mixed with FLAG-E1 in the presence of 50 μM **1**, **2**, **7**, or 0.5% DMSO as a positive control, and the mixture was subjected to immunoprecipitation (IP) with anti-GST antibody-immobilized beads and to SDS–PAGE, followed by Western blotting with anti-FLAG antibody. Input, FLAG-E1 only; control, a negative control without FLAG-E1. (B) A model for three steps of the E1-catalyzed ubiquitin-activation reaction. **7** inhibits the binding of ubiquitin to the binding site in E1, while **1** and **2** cannot inhibit the ubiquitin binding but may inhibit the formation of the ubiquitin-adenylate intermediate or/and that of the ubiquitin–cysteine thioester intermediate. Ub, ubiquitin; PPi, pyrophosphate; SH, a sulfhydryl group of the active cysteine residue.

of E1, in contrast to **7** (Fig. 4 (B)). Compound **7**, isolated from a marine-derived fungus, inhibits E1 with an IC_{50} value of approximately 50 μM.[8] Thus, **1** and **2** inhibit E1 more strongly than **7** and in a manner different from **7**.

3. Discussion

In this paper, we isolated three epimeric pairs of alkaloids, **1**/**2**, **3**/**4**, and **5**/**6**, in which **1**, **2**, and **5** were new tetrahydro-β-carboline alkaloids, and **3** and **4** were new azepinoindole-type alkaloids. Interestingly, **1** and **2** inhibited E1 with IC_{50} values of 2.4 and 35 μM, respectively. Thus, **1** is the strongest E1 inhibitor among natural E1 inhibitors isolated so far, **2**, **7**, panapophenanthorine (**8**) (with an IC_{50} of 40 μM[9]), and largazole (**9**) (with an IC_{50} of 29 μM[10]) (Fig. 5). It should be noted that **1**–**6** showed little cytotoxicity against HeLa cells even at 50 μg/mL. Although **1** is a potent E1 inhibitor in vitro, this compound might be impermeable to the cells.

Possibly, **3**–**6** would be biosynthesized by the Pictet-Spengler reaction with L-tryptophan and L-alanine (Scheme 1).[20] The condensation of L-tryptophan and L-alanine would afford an iminium ion, followed by nucleophilic attack in two distinct reaction sequences, pathways A and B, and subsequent cyclization to afford **3**/**4** and **5**/**6**, respectively. Alternatively, the condensation of L-tryptophan and L-histidine would afford **1** and **2** in the same way. While *trans/cis* ratios differ greatly among the three pairs of isolates, 0.67 (**1**/**2**), 0.53 (**3**/**4**), and 0.041 (**5**/**6**), thermodynamically unstable *cis* isomers are dominant for these pairs. The mechanisms of the Pictet-Spenglerases, which would catalyze the condensation of two amino acids, toward the above metabolites are interesting. Although, numerous metabolites probably biosynthesized by the Pictet-Spengler reaction have been reported, the few azepinoindole derivatives were isolated from natural sources, including an epimeric mixture of clavicipitic acid (**10**) (Fig. 6) from cultures of *Claviceps* strain SD 58[21] and *C. fusiformis* 139/2/1G[22] and hyrtiazepine[23] (**11**) from the Red Sea marine sponge *Hyrtios erectus*. However, as metabolites derived from tryptophan and histidine, lissoclin C[24] (**12**) and haploscleridamine[25] (**13**) were isolated from a tropical ascidian *Lissoclinum* sp. and a sponge of the order Haplosclerida, respectively.

The ubiquitin–proteasome system controls a wide range of cellular events including cell-cycle progression, and defects associated with this system result in various diseases including cancer and neurodegenerative disorders. Thus, the ubiquitin–proteasome system is emerging as a significant target in anticancer therapies. Bortezomib, a synthetic proteasome inhibitor, is already on the market for the treatment of patients with relapsed multiple myeloma and is also undergoing clinical trials for other cancers. In preclinical studies, bortezomib showed antitumor activity against a variety of solid tumors, including breast, gastric, colon, pancreas, and non-small lung cancers.[26] In addition, nowadays, inhibitors targeting the ubiquitin system including E1, E2, and E3 enzymes, the delivery system, and deubiquitinating enzymes are also

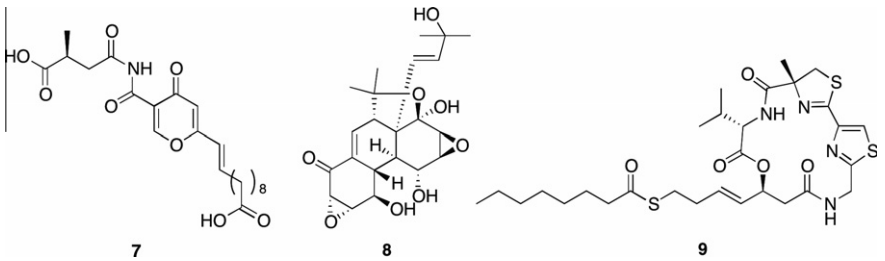

Figure 5. Structures of natural E1 inhibitors, himeic acid A (**7**), panepophenanthrine (**8**), and largazole (**9**).

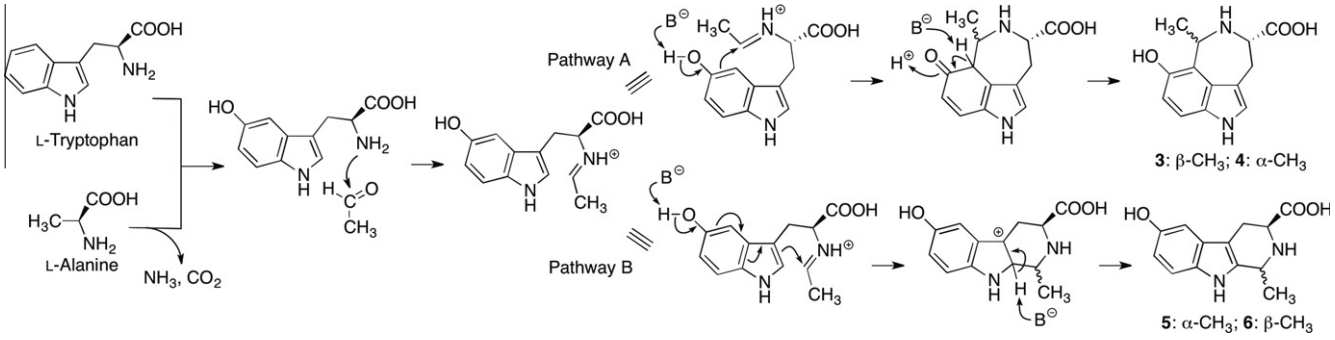

Scheme 1. A possible biogenetic pathway for hyrtioreticulins C–E (**3**–**5**) and hyrtioerectine B (**6**).

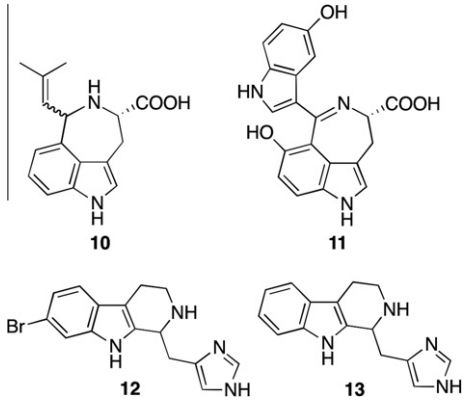

Figure 6. Structures of natural compounds probably biosynthesized by the Pictet-Spengler reaction, including clavicipitic acid (**10**), hyrtiazepine (**11**), lissoclin C (**12**), and haploscleridamine (**13**).

candidates for anticancer drugs, and several compounds are now undergoing preclinical and clinical trials for cancers.[27–29] The development of E1 inhibitors by searching natural sources and chemical libraries and also by chemical synthesis is needed to develop efficient anticancer drugs and to investigate the complex ubiquitin–proteasome system.

4. Experimental

4.1. General experimental procedures

Optical rotations were determined with a JASCO DIP-1000 polarimeter in MeOH. UV spectra were measured on a JASCO V-550 spectrophotometer in MeOH. CD spectra were measured on a JASCO J-820 spectropolarimeter in MeOH at 24 °C. IR spectra were measured on a JEOL JIR-6500 W spectrophotometer. NMR spectra were recorded on a Bruker Avance 500 NMR spectrometer in CD_3OD or DMSO-d_6. Chemical shifts were referenced to the residual solvent peaks (δ_H 3.30 and δ_C 49.0 for CD_3OD; δ_H 2.49 and δ_C 39.5 for DMSO-d_6), and multiplicities of carbon resonances were determined from HMQC spectra. Mass spectra were measured on a JEOL JMS-700, BRUKER esquire 3000plus-K1, or BRUKER micrOTOFII mass spectrometer.

4.2. Biological material

The marine sponge was collected at a depth of 10 m in North Sulawesi, Indonesia, in September 2006 and soaked in EtOH immediately. The sponge was identified as *H. reticulatus*. A voucher specimen (RMNH POR 3989) has been deposited in Netherlands Centre for Biodiversity Naturalis, The Netherlands.

4.3. Extraction and isolation

The marine sponge was extracted with EtOH. The concentrated aqueous residue was successively extracted with EtOAc and *n*-BuOH. The *n*-BuOH fraction (9.55 g) was subjected to silica gel column chromatography with $CHCl_3$/MeOH and $CHCl_3$/MeOH/H_2O to afford fractions A–C. Fraction A (1.02 g) eluted with $CHCl_3$/MeOH/H_2O (7:3:0.5) was purified by ODS column chromatography with 10% and 30% CH_3CN–H_2O followed by HPLC (Phenomenex Phenyl-hexyl column with 10% CH_3CN–H_2O (0.01% TFA)) to afford hyrtioreticulins C (**3**, 11.0 mg, 0.0028% wet weight), D (**4**, 20.9 mg, 0.0052%), and E (**5**, 10.4 mg, 0.0026%) along with hyrtioerectine B (**6**, 7.5 mg, 0.0019%). Fraction B (1.51 g), which was eluted with $CHCl_3$/MeOH/H_2O (6:4:1), yielded **6** (247.9 mg, 0.062%) as colorless needles directly from the solution. Fraction C (2.99 g) eluted with $CHCl_3$/MeOH/H_2O (6:4:1 and 5:5:1) was purified by ODS column chromatography with 10% CH_3CN–H_2O followed by HPLC (Phenomenex Phenyl-hexyl column with 10% CH_3CN–H_2O (0.05% TFA) and COSMOSIL πNAP column with 10% CH_3CN–H_2O (0.05% TFA)) to afford hyrtioreticulins A (**1**, 4.0 mg, 0.0010%) and B (**2**, 6.0 mg, 0.0015%).

4.4. Hyrtioreticulin A (1)

$[\alpha]_D^{25}$ +23.8° (*c* 1.35, MeOH); UV (MeOH) λ_{max} (log ε) 309 (3.42), 274 (3.67), 210.5 (4.16); IR (film) ν_{max} 3357, 3147, 2852, 1675, 1629, 1390, 1205, 1133, 1081, 838, 800, 719, 667 cm^{-1}; ^1H and ^{13}C NMR data, see Table 1; positive ESIMS *m/z* 313 $[M+H]^+$. HRESIMS *m/z* 313.1300 (Calcd for $C_{16}H_{17}N_4O_3$, 313.1301).

4.5. Hyrtioreticulin B (2)

$[\alpha]_D^{25}$ −49.2° (*c* 0.90, MeOH); UV (MeOH) λ_{max} (log ε) 307.5 (3.54), 273 (3.75), 208.5 (4.21); IR (film) ν_{max} 3293, 3116, 2921, 1675, 1619, 1413, 1394, 1203, 1139, 838, 800, 723, 667 cm^{-1}; ^1H and ^{13}C NMR data, see Table 1; positive ESIMS *m/z* 313 $[M+H]^+$. HRESIMS *m/z* 313.1297 (Calcd for $C_{16}H_{17}N_4O_3$, 313.1301).

4.6. Hyrtioreticulin C (3)

$[\alpha]_D^{25}$ +17.6° (*c* 0.47, MeOH); UV (MeOH) λ_{max} (log ε) 304 (3.43), 280 (3.48), 211(3.95); IR (film) ν_{max} 3214, 2992, 1672, 1633, 1583, 1419, 1373, 1313, 1271, 1248, 1200, 1168, 1133, 1020, 941, 833, 800, 721 cm^{-1}; ^1H and ^{13}C NMR data, see Table 2; positive FABMS *m/z* 247 $[M+H]^+$; positive HRFABMS *m/z* 247.1063 (Calcd for $C_{13}H_{15}N_2O_3$, 247.1082).

4.7. Hyrtioreticulin D (4)

$[\alpha]_D^{25}$ −117.5° (*c* 0.55, MeOH); UV (MeOH) λ_{max} (log ε) 302 (3.35), 280 (3.42), 211(3.93); IR (film) ν_{max} 3214, 2921, 1674, 1635, 1592,

1436, 1374, 1314, 1275 1250, 1200, 1185, 1132, 1015, 949, 832, 799, 721 cm^{-1}; ^1H and ^{13}C NMR data, see Table 2; positive FABMS *m/z* 247 $[M+H]^+$; positive HRFABMS *m/z* 247.1075 (Calcd for $C_{13}H_{15}N_2O_3$, 247.1082).

4.8. Hyrtioreticulin E (5)

$[\alpha]_D^{25}$ −11.2° (*c* 0.28, MeOH); UV (MeOH) λ_{max} (log ε) 272 (3.23), 224 (3.60), 209 (3.63) nm; IR (film) ν_{max} 3227, 2361, 2334, 1674, 1635, 1456, 1398, 1201, 1145, 841, 802, 722 cm^{-1}; ^1H and ^{13}C NMR data, see Table 3; FABMS *m/z* 247 $[M+H]^+$; HRFABMS *m/z* 247.1086 (Calcd for $C_{13}H_{15}N_2O_3$, 247.1082).

4.9. Hyrtioerectine B (6)

$[\alpha]_D^{25}$ −59.4° (*c* 0.57, MeOH).

4.10. Measurement of E1 activity

E1 activity was measured on the basis of the formation of the E1-ubiquitin intermediate from E1 and ubiquitin in the presence of ATP. FLAG-tagged E1[19] (0.1 μg) was previously incubated at 37 °C for 30 min in 25 μL of a reaction mixture containing 50 mM Tris–HCl, pH 7.6, 0.1 mM dithiothreitol, 10 mM $MgCl_2$, 2 mM ATP, and 0.25 units of inorganic pyrophosphatase (SIGMA–ALDRICH). Subsequently 0.5 μg of GST-ubiquitin (MBL) was added and the resulting mixture was incubated at 37 °C for 60 min. The reaction was terminated by the addition of SDS loading buffer and the reaction mixture was subjected to SDS–PAGE in a slab gel containing 9% polyacrylamide under non-reducing conditions. After the proteins were blotted to nitrocellurose membranes (BIO-RAD), blocking with 5% skim milk in phosphate-buffered saline containing 0.1% Tween 20 and subsequent immunoblotting were carried out. For immunochemical detection of FLAG-tagged E1, a mouse monoclonal M2 antibody against FLAG-tag (SIGMA–ALDRICH) and peroxidase-conjugated anti-mouse IgG (GE Healthcare) were used as the first and second antibodies, respectively. Detection was performed using an enhanced chemiluminescence system (Wako Pure Chemical Industries, Ltd.), and bands were visualized with a FUJIFILM luminescent image analyzer, Fuji LAS-3000mini (Fuji Photo Film Co., Ltd.).

4.11. Immunoprecipitation (IP) experiment

Anti-GST monoclonal antibody (MBL) (1.6 μg) was incubated with protein G-immobilized agarose beads (25 μL) in phosphate-buffered saline containing 0.1% Tween 20 for 10 min at 20 °C. In the presence or absence of 50 μM E1 inhibitor, anti-GST antibody-immobilized beads were mixed with GST-ubiquitin (1.5 μg) and FLAG-tagged E1 (1.4 μg) in 200 μL of IP buffer containing 50 mM Tris–HCl, pH 7.6, 100 mM NaCl, 10 mM $MgCl_2$, 0.5 mM EDTA, 2% glycerol, and 0.25% NP-40, and then incubated at 20 °C for 20 min. After four washes with IP buffer, the beads were suspended in SDS–PAGE loading buffer (30 μL) and subjected to SDS–PAGE on a 7.5% polyacrylamide gel, followed by Western blotting with anti-FLAG M2 antibody conjugated with peroxidase.

Acknowledgments

We thank Dr. H. Kobayashi of the University of Tokyo and Dr. Kazuyo Ukai of Tohoku Pharmaceutical University for collection of the sponge. This work was financially supported by Grants-in-Aid from the Ministry of Education, Culture, Sports, Science and Technology of Japan (Nos. 22310138 and 22406001) and also by grants from the Naito Foundation, the Astellas Foundation for Research on Metabolic Disorders, and the Uehara Memorial Foundation.

Supplementary data

Supplementary data associated with this article can be found, in the online version, at http://dx.doi.org/10.1016/j.bmc.2012.05.044.

References and notes

1. Hershko, A.; Ciechanover, A. *Annu. Rev. Biochem.* **1998**, *67*, 425.
2. Glickman, M. H.; Ciechanover, A. *Physiol. Rev.* **2002**, *82*, 373.
3. Voges, D.; Zwickl, P.; Baumeister, W. *Annu. Rev. Biochem.* **1999**, *1015*, 68.
4. Pickart, C. M. *Annu. Rev. Biochem.* **2001**, *70*, 503.
5. Finley, D. *Annu. Rev. Biochem.* **2009**, *78*, 477.
6. Tanaka, K. *Proc. Jpn. Acad. B: Phys. Biol. Sci.* **2009**, *85*, 12.
7. Adams, J. *Drug Discovery Today* **2003**, *8*, 307.
8. Tsukamoto, S.; Hirota, H.; Imachi, M.; Fujimuro, M.; Onuki, H.; Ohta, T.; Yokosawa, H. *Bioorg. Med. Chem. Lett.* **2005**, *15*, 191.
9. Sekizawa, R.; Ikeno, S.; Nakamura, H.; Naganawa, H.; Matsui, S.; Iinuma, H.; Takeuchi, T. *J. Nat. Prod.* **2002**, *65*, 1491.
10. Ungermannova, D.; Parker, S. J.; Nasveschuk, C. G.; Wang, W.; Quade, B.; Zhang, G.; Kuchta, R. D.; Phillips, A. J.; Liu, X. *PLoS ONE* **2012**, *7*, e29208.
11. Yang, Y.; Kitagaki, J.; Dai, R. M.; Tsai, Y. C.; Lorick, K. L.; Ludwig, R. L.; Pierre, S. A.; Jensen, J. P.; Davydov, I. V.; Oberoi, P.; Li, C. C.; Kenten, J. H.; Beutler, J. A.; Vousden, K. H.; Weissman, A. M. *Cancer Res.* **2007**, *67*, 9472.
12. Ungermannova, D.; Parker, S. J.; Nasveschuk, C. G.; Chapnick, D. A.; Phillips, A. J.; Kuchta, R. D.; Liu, X. *J. Biomol. Screen.* **2012**, *17*, 421.
13. Youssef, D. T. A. *J. Nat. Prod.* **2005**, *68*, 1416.
14. Teitel, S.; Brossi, A. *Lloydia* **1974**, *37*, 196.
15. Haas, A. L.; Warms, J. V. B.; Hershko, A.; Rose, I. A. *J. Biol. Chem.* **1982**, *257*, 2543.
16. Walden, H.; Podgorski, M. S.; Schulman, B. A. *Nature* **2003**, *422*, 330.
17. Lee, I.; Schindelin, H. *Cell* **2008**, *134*, 268.
18. Schulman, B. A.; Harper, J. W. *Nat. Rev. Mol. Cell Biol.* **2009**, *10*, 319.
19. Saeki, Y.; Tayama, Y.; Toh-e, A.; Yokosawa, H. *Biochem. Biophys. Res. Commun.* **2004**, *320*, 840.
20. Stöckigt, J.; Antonchick, A. P.; Wu, F.; Waldmann, H. *Angew. Chem., Int. Ed.* **2011**, *50*, 8538.
21. Robbers, J. E.; Otsuka, H.; Floss, H. G. *J. Org. Chem.* **1980**, *45*, 1117.
22. King, G. S.; Waight, E. S.; Mantle, P. G.; Szczyrbak, C. A. *J. Chem. Soc., Perkin Trans. 1* **1977**, 2099.
23. Sauleau, P.; Martin, M. T.; Dau, M. E.; Youssef, D. T.; Bourguet-Kondracki, M. L. *J. Nat. Prod.* **2006**, *69*, 1676.
24. Searle, P.; Molinski, T. F. *J. Org. Chem.* **1994**, *59*, 6600.
25. Patil, A. D.; Freyer, A. J.; Carte, B.; Taylor, P. B.; Johnson, R. K.; Faulkner, D. J. *J. Nat. Prod.* **2002**, *65*, 628.
26. Milano, A.; Iaffaioli, R. V.; Caponigro, F. *Eur. J. Cancer* **2007**, *43*, 1125.
27. Bedford, L.; Lowe, J.; Dick, L. R.; Mayer, R. J.; Brownell, J. E. *Nat. Rev. Drug Disc.* **2011**, *10*, 29.
28. Cohen, P.; Tcherpakov, M. *Cell* **2010**, *143*, 686.
29. Ande, S. R.; Chen, J.; Maddika, S. *Eur. J. Pharmacol.* **2009**, *625*, 199.